

OBSERVATION OF THE MICROQUASAR LS 5039 WITH H.E.S.S.

M. de Naurois¹ and the H.E.S.S. collaboration

Abstract. The High Energy Stereoscopic System (H.E.S.S.) is an array of four imaging atmospheric-Cherenkov telescopes located in the Khomas Highlands of Namibia. The microquasar LS 5039 was serendipitously detected by the instrument during the scan of the inner galactic plane in 2004. Deeper observation were carried out in 2005, and brought a clear evidence for TeV emission variability. This is after PSRB 1259-63 the second VHE gamma-rays variable galactic source discovered. We will present detailed studies of the source variability (flux and spectral shape) compared to other wavelenghtes and shortly review the implications for the existing emission models.

1 Introduction

In the commonly accepted paradigm, microquasars consist of a stellar mass black hole fed by a massive star. They can exhibit superluminous radio jets (Mirabel & Rodriguez 1994), and hints for the presence of an accretion disk. LS 5039, identified by Motch et al (1997) as a massive X-ray binary system with faint radio emission (Marti et al. 1998), was resolved by Paredes et al. (2000) into bipolar mildly relativistic radio jets ($v \sim 0.2 c$) emanating from a central core, thus placing it into the *microquasar class*. The detection of radio and variable X-ray emission (Bosch-Ramon et al. 2005) and its possible association with the EGRET source 3EG J1824-1514 suggested the presence of multi-GeV particles accelerated in jets. This binary system (Fig 1) consists of a massive O6.5V star in a ~ 3.9 day mildly eccentric orbit ($e = 0.35$)(Casares et al. 2005) around a compact object whose exact nature (black hole or neutron star) is still under debate.

2 H.E.S.S. Observations

The High Energy Stereoscopic System (H.E.S.S.) is an array of four identical Atmospheric Cherenkov Telescopes (ACT)(Aharonian et al. 2006a) located in the Southern Hemisphere (Namibia, 1800 m a.s.l.) and sensitive to γ -rays above 100 GeV. LS 5039 was serendipitously detected in 2004 during the H.E.S.S. galactic scan (Aharonian et al. 2005a). The 2004 observations have been followed up by a deeper observation campaign (Aharonian et al. 2006b) in 2005, leading to a total dataset of 69.2 hours of observation after data quality selection. Data were analysed using two separate calibrations (Aharonian et al. 2004) and analysis pipelines. The results presented here are based on the log-likelihood comparison of the shower images with a precalculated semi-analytical model (de Naurois et al. 2005).

After selection cuts, a total of 1969 γ -ray events were found within 0.1° of the VLBA radio position of LS 5039, leading to a statistical significance of 40σ (Fig. 2). The best fit position is, in Galactic Coordinates, $l = 16.879^\circ$, $b = -1.285^\circ$ with statistical and systematic uncertainties of respectively $\pm 12''$ and $\pm 20''$. It is compatible with the VLBA position (denoted as a blue star in Fig. 2). We obtain an upper limit of $28''$ (at 1σ) on the VHE source extension.

2.1 Timing Analysis

The runwise VHE γ -ray flux at energies ≥ 1 TeV was decomposed into its frequency components using the Lomb-Scargle periodogram (Scargle 1982) (Fig. 3) which is appropriate for unevenly sampled datasets such as

¹ Laboratoire de Physique Nucléaire et de Hautes Energies, 4 place Jussieu, 75252 Paris Cedex 05

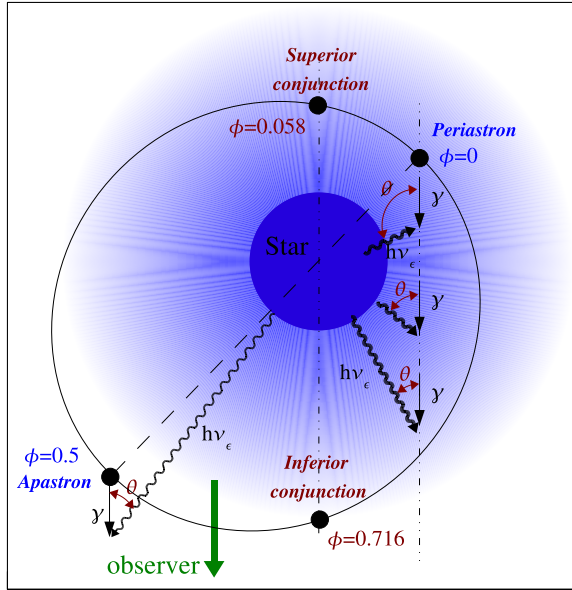


Fig. 1. Orbital geometry of the binary system LS 5039 viewed from above and using the orbital parameters derived by Casares et al. (2005). Shown are: phases (ϕ) of minimum (*periastron*) and maximum (*apastron*) binary separation; epoch of superior and inferior conjunctions occurring when the compact object and the star are aligned along the observer light-of-sight.

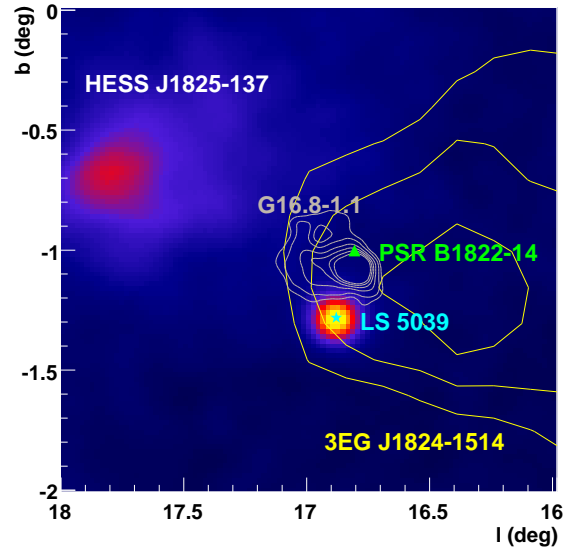


Fig. 2. H.E.S.S. excess sky map around LS 5039, smoothed by the instrument point spread function. The blue star denotes the position of the VLBA source. The yellow contours correspond to the 68%, 95% and 99% confidence level region of the EGRET source 3EG J1824-1514. The extended source HESS J1825-137 observed in the same field of view can serve as a cross-check for timing-analysis.

those collected by H.E.S.S. A very significant peak (chance probability of $\sim 10^{-20}$ before trials) occurs in the Lomb-Scargle periodogram at the period 3.9078 ± 0.0015 days, consistent with the orbital period determined by Casares et al. (2005) (3.90603 ± 0.00017). The effect of subtracting a pure sinusoid at the orbital period is shown in Fig. 3, middle panel. The orbital peak disappears as expected, but also the numerous satellite peaks with chance probabilities less than 10^{-7} - 10^{-8} that were present in the original periodogram. These peaks are beat periods of the orbital period with the various gaps present in the H.E.S.S. dataset (day-night cycle, moon period, annual period). The bottom panel of the same figure shows the result obtained on the neighbouring source HESS J1825-137 observed in the same field of view as LS 5039, which doesn't show any statistically significant peak, thus demonstrating that the observed periodicity is genuinely associated with LS 5039.

2.2 Flux Modulation

The runwise Phasogram (Fig. 4) of integral flux at energies ≥ 1 TeV vs. orbital phase (ϕ) shows an almost sinusoidal behaviour, with the bulk of the emission largely confined in a phase interval $\phi \sim 0.45$ to 0.9 , covering about half of the orbital period. The emission maximum ($\phi \sim 0.7$) appear to lag behind the apastron epoch and to align better with the *inferior conjunction* ($\phi = 0.716$), when the compact object lies in front of the massive star (see Fig. 1). The VHE flux minimum occurs at phase ($\phi \sim 0.2$), slightly further along the orbit than *superior conjunction* ($\phi = 0.058$). Neither evidence for long-term secular variations in the VHE flux independent of the orbital modulation nor any other modulation period are found in the presented H.E.S.S. data.

2.3 Spectral Modulation

Due to changing environment with orbital phase (magnetic field strength, stellar photon field, relative position of compact object and star with respect to observer, ...), the VHE γ -ray emission spectrum is expected to vary along the orbit. We first define two broad phase interval: **INFC** centered on the inferior conjunction

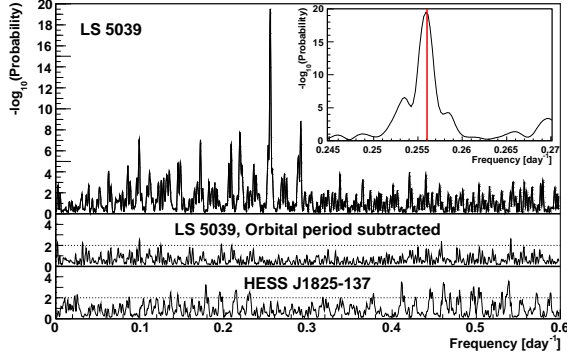


Fig. 3. Lomb-Scargle (LS) periodogram of the VHE run-wise flux of LS 5039 above 1 TeV (Chance probability to obtain the LS power vs. frequency). From Aharonian et al (2006b). Zoom: inset around the highest peak, which corresponds to a period of 3.9078 ± 0.0015 days. This period is found to be compatible with the orbital period determined by Casares et al. (2005) and denoted as a red line on the inset. Middle: LS periodogram of the same data after subtraction of a pure sinusoidal component at the orbital period of 3.90603 days (see text). Bottom: LS periodogram obtained on HESS J1825-137 observed in the same field of view.

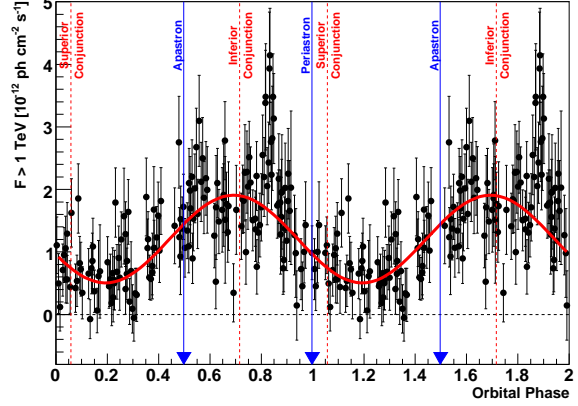


Fig. 4. Phasogram (Integral run-by-run γ -ray flux above 1 TeV as function of orbital phase) of LS 5039 from H.E.S.S. data from 2004 to 2005, using the orbital ephemeris of Casares et al. (2005). Each run is ~ 28 minutes. Two full phase periods are shown for clarity. The vertical blue arrows depict the respective phases of minimum (*periastron*) and maximum (*apastron*) binary separation. The vertical dashed red lines show the respective phases of inferior and superior conjunction, when the star and the compact object are aligned along the observer's line of sight. From Aharonian et al (2006b).

($0.45 < \phi \leq 0.9$) and its complementary **SUPC** centered on the superior conjunction, corresponding respectively to high and low flux states. The high state VHE spectral energy distribution (Fig. 5) is consistent with a hard power law with index $\Gamma = 1.85 \pm 0.06_{\text{stat}} \pm 0.1_{\text{syst}}$ and exponential cutoff at $E_0 = 8.7 \pm 2.0$ TeV. In contrast, the spectrum for low state is compatible with a relatively steep ($\Gamma = 2.53 \pm 0.06_{\text{stat}} \pm 0.1_{\text{syst}}$) pure power law extending from 200 GeV to ~ 20 TeV. Interestingly, the flux appears to be almost unmodulated at 200 GeV as well as around 20 TeV, whereas the modulation is maximum around a few (~ 5) TeV.

Trying to go to smaller phase interval, Fig. 6 shows the results (photon index and differential flux at 1 TeV) of a pure power-law fit of the high energy spectra in 0.1 orbital phase bins (restricted to energies below 5 TeV to avoid systematic effect introduced by the high state cutoff). The flux normalisation and photon index are strongly correlated, the flux being higher when the spectrum is harder and vice-versa. Interestingly, a similar effect, however in a smaller variation range and a different phasogram, was found in X-rays (Bosch-Ramon et al. 2005).

3 Interpretation and Conclusion

The basic paradigm of VHE γ -ray production requires the presence of particles accelerated to multi-TeV energies and a target comprising photons (for γ -ray production through Inverse Compton effect) and/or matter of sufficient density (for γ -ray production through pion decay in hadronic processes).

New observations by HESS have established orbital modulation of the VHE γ -ray flux and energy spectrum from the XRB LS 5039. The observed VHE modulation indicates that the emission most probably takes place close (within ~ 1 AU) to the massive stellar companion, where modulated γ -ray absorption via pair production (e^+e^-) on the intense stellar photon field is unavoidable (e.g. Dubus, 2006). The observed spectral modulation is however incompatible with a pure absorption scenario, which in particular predicts a maximum variability around 300 GeV and a VHE spectral hardening in the low flux state, inconsistent with observations.

Modulation could also arise from a modulation of the acceleration and cooling timescales along the orbit due to varying magnetic field and photon field densities (e.g. Aharonian et al. 2006b), and possibly from modulation of the accretion rate in the microquasar scenario (e.g. Paredes et al. 2006).

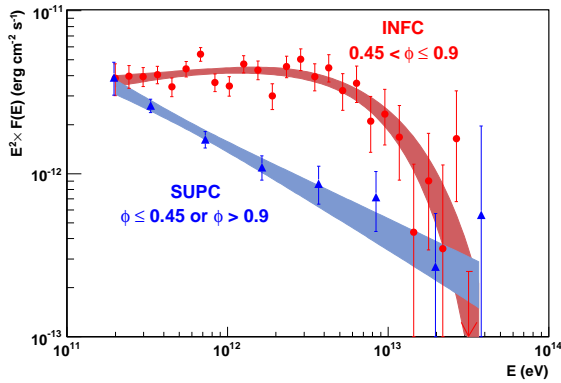


Fig. 5. Very high energy spectral energy distribution of LS 5039 for the two broad orbital phase intervals defined in the text, **INFC** (red circles) and **SUPC** (blue triangles). The shaded regions represent the 1σ confidence bands on the fitted functions. A clear spectral hardening is occurring in the 200 GeV to a few TeV range during the **INFC** phase interval. From 3.

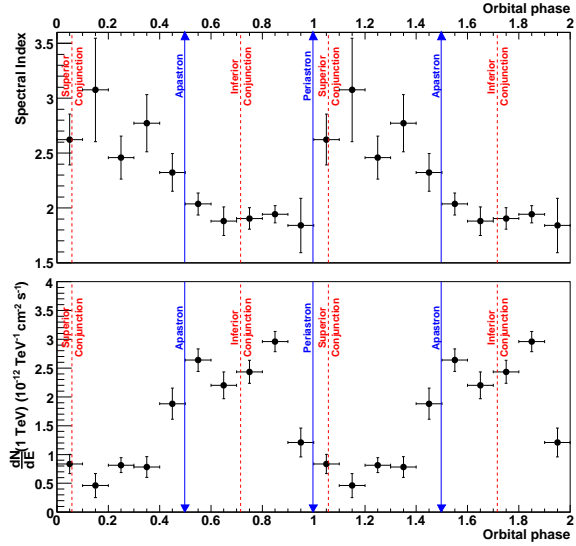


Fig. 6. Top: Fitted pure power-law photon index vs. phase interval of width $\Delta\phi = 0.1$. Bottom: Differential flux at 1 TeV for the same phase interval. From 3.

A detailed study is now required to fully explain these new observations and understand the complex relationship between γ -ray absorption and production processes within these binary systems.

The support of the Namibian authorities and of the University of Namibia in facilitating the construction and operation of H.E.S.S. is gratefully acknowledged, as is the support by the German Ministry for Education and Research (BMBF), the Max Planck Society, the French Ministry for Research, the CNRS-IN2P3 and the Astroparticle Interdisciplinary Programme of the CNRS, the U.K. Particle Physics and Astronomy Research Council (PPARC), the IPNP of the Charles University, the South African Department of Science and Technology and National Research Foundation, and by the University of Namibia. We appreciate the excellent work of the technical support staff in Berlin, Durham, Hamburg, Heidelberg, Palaiseau, Paris, Saclay, and in Namibia in the construction and operation of the equipment.

References

- Aharonian, F., et al. (HESS Collaboration) 2004, *Astropart. Phys.* 22 109-125
 Aharonian, F., et al. (HESS Collaboration) 2005a, *Science* 309, 746
 Aharonian, F., et al. (HESS Collaboration) 2006b, *A&A*, in press and astro-ph/0607192
 Aharonian, F., et al. (HESS Collaboration) 2006a, *A&A*, in press and astro-ph/0607333
 Bosch-Ramon V. et al. 2005, *ApJ.* 628, 388
 Casares, J. et al. 2005 *MNRAS* 364, 899
 de Naurois M., et al., 2005 *Proc. Towards a Network of Atmospheric Cherenkov Detectors VII* (Palaiseau) p.149.
 Dubus, G. 2006, *A&A* 451, 9-18
 Martí, J., Paredes, J. M., Ribó, M. 1998, *A&A* 338, L71-L74
 Mirabel, I.F., Rodríguez L.F. 1994 *Nature* 371, 46
 Motch, C., et al. 1997, *A&A* 323 853-875
 Paredes, J.M., Martí J., Ribó M., Massi M. 2000, *Science* 288, 2340
 Paredes, J.M., Bosch-Ramon V., Romero G.E. 2006, *A&A* 451, 259
 Scargle, J.D. 1982, *ApJ* 263, 835